Compact Dual-Band PCML-SIR Bandpass Filters with Edge-Capacitive Coupling

#Jayaseelan Marimuthu and Mazlina Esa
Faculty of Electrical Engineering, Universiti Teknologi Malaysia
81310 UTM Skudai, Johor, Malaysia, jayaseelan.marimuthu@yahoo.com, mazlina@fke.utm.my

1. Introduction

In recent years, compact multiband devices compatible with printed circuit board (PCB), have received great demand for advanced wireless systems with simultaneous operations at multiple frequency bands. With the advent of wireless communications, the design of many passive circuits such as the bandpass filters, are facing new design challenges including compact in size, wide bandwidth and multi-band operations. High data-rate wireless communication systems, such as worldwide interoperability for microwave access (WiMAX) and wireless local area network (WLAN), require wide bandwidth up to several hundred of megahertz and flexibility of operating in multiple frequency bands. Planar bandpass filters fabricated on printed circuit board (PCB) are attractive for filter application because their low fabrication cost suits commercial application well [1–2]. The multi-band microwave components, when realized, can lead to both the size and cost reduction in the circuits used for multi-band wireless communication systems [3–4].

In this paper, a simple dual-band bandpass filter were constructed by cascading the multiple $\lambda/2$ stepped-impedance resonators (SIRs) through the distributed parallel coupled microstrip lines (PCMLs) with edge-capacitive coupling configuration. It is named PCML-SIR ECC filter. A simple PCML structure with high impedance feeding network shows dual-band characteristics. Similarly a SIR cascaded with PCML coupling also shows dual-band response. A single-stage dual-band bandpass filter was designed by cascading a simple SIR structure coupled with PCML of high impedance feeding network. The single-stage dual-band filter passband response and bandwidth are adjustable by controlling the impedance ratio of both strips and middle resonator length of SIR and also the impedance of PCML feeding network. The edge-capacitive coupling technique was introduced and incorporated in PCML-SIR filter to obtain good stopband response between two passband. The stopband response between two resonant frequencies depends on the gap of edge-capacitive coupling between two PCML structures. By suitably choosing edge-capacitive coupling gap, a perfect stopband response with two transmissions zero can be obtained between the two resonant frequencies. Various PCML-SIR single-stage dual-band bandpass filters were designed on RT/duroid 6006 of ε_r = 6.15 and h =1.27 mm to investigate the performance of filter in terms of bandwidth and stopband characteristics. Finally, three two-stage dual-band bandpass filters of PCML-SIR ECC are optimally designed and fabricated to demonstrate in reality the dual-band performance with controllable bandwidth and stopband parameters. It was found that the simulated and measured insertion and return losses responses showed good agreement with excellent stopband performance with two transmission zero frequencies.

2. PCML Structure with Dual-Band Characteristics

A simple PCML structure with various feeding network width has been designed to investigate the performance of structure as shown in Figure 1(a). The two-port admittance *Y*-matrix of the PCML design effectively extracted using full-wave analysis of commercially available *em* tools. Since the *J*-inverter network with the susceptance (*J*) and two equal electrical length of $\theta/2$ at the two sides can be modeled equivalent to PCML, the equivalent circuit of a two-port network admittance of PCML can be used to calculate the *J*-susceptance and electrical length (θ) [5]. Figure 2 shows the computed normalized *J*-inverter susceptance $\overline{J}$ of a PCML structure with various feeding network width. It shows that as w_o decreases from 1.9 mm to 0.3 mm, the $\bar{J}$ susceptance shows dual-band performance. Initially when w_o = 1.9 mm, single band appeared at f_o = 5.5 GHz, as the w_o decreases two-band present at f_o = 3 GHz and f_1 = 9.5 GHz. When w_o = 0.7 mm, both bands have almost the same susceptance $\bar{J}$ value with similar bandwidth with equivalent coupling degree. As w_o further decreases, the coupling degree of PCML weakens at the first operating band and strengthens at the second operating band. This result demonstrates that PCML structure with feeding network of higher value of characteristic impedance has the dual-band characteristics. The bandwidth of both bands can be freely tuned by adjusting the width of feeding network. It clearly shows that this technique can be further used to enhance the bandwidth of second resonant frequency.

3. Single-Stage Dual-Band PCML-SIR Filter

Single-stage microstrip dual-band bandpass filter was designed by using a simple SIR structure coupled with high impedance feeding network PCML structure as shown in Figure 3. A simple SIR structure has dual-band characteristics. Its resonant frequencies separation depend on the aspect ratio of the two impedances $R_Z = Z_2/Z_1$ and length ratio (L_1/L_2) of the two side sections in SIR structure as shown in Figure 3(a). The separation of resonant frequencies was carefully selected based on specific value of R_Z and L_1/L_2 such that the resonant frequencies by the SIR fall within the region of the PCML resonant frequency as shown in Figure 2. The edge capacitive coupling configuration method was introduced in this design to improve the stopband response of the filter.

Various configurations of single-stages dual-band bandpass filter as shown in Figure 3(b) were designed to investigate the behavior of filter respect to R_Z (W_g) and L_c. The design parameters are w_o = w_c =0.7 mm, L_1 = L_2 = 7.0 mm, L_{g2} = L_c and L_{g1} = 0.4 mm. The results show that as R_Z decreases both resonant frequencies approach each other. By increasing the length L_c both resonant frequencies will be shifted to lower frequency. These two parameters can be used effectively to select suitable operating frequencies for the dual-band bandpass filter. In this design, the resonant frequencies f_o = 4.25 GHz and f_1 = 9.25 GHz were set as the operating frequencies by choosing R_Z = 1.3 (w_g = 0.3 mm) and L_c = 2.1 mm.

Using the above physical parameters, four single-stages dual-band bandpass filter as shown in Figure 3(b) with various feeding network width (impedance) were design. Its S_{21}-magnitude under the four different feeding network width is simulated and plotted in Figure 4 to demonstrate the behavior of the filter on dual-band bandpass bandwidth at f_o = 4.25 GHz and f_1 = 9.25 GHz. In this case, the bandwidth observes for w_o = 1.9 mm is 800 MHz (at f_o = 4.25 GHz) and 200 MHz (at f_1 = 9.25 GHz), w_o = 1.0 mm is 750 MHz (at f_o = 4.25 GHz) and 400 MHz (at f_1 = 9.25 GHz), w_o = 0.7 mm is 600 MHz (at f_o = 4.25 GHz) and 600 MHz (at f_1 = 9.25 GHz) and w_o = 0.5 mm is 500 MHz (at f_o = 4.25 GHz) and 750 MHz (at f_1 = 9.25 GHz) as shown in Figure 4. It shows clearly that the bandwidth of the dual passbands can be freely adjusted to well realize the four distinctive dual-band cases, as listed in the following equations:

$$\text{BW at } f_o = 4.25 \text{ GHz} > \text{BW at } f_1 = 9.25 \text{ GHz, for } w_o = 1.9 \text{ mm} \quad (1)$$

$$\text{BW at } f_o = 4.25 \text{ GHz} = \text{BW at } f_1 = 9.25 \text{ GHz, for } w_o = 0.7 \text{ mm} \quad (2)$$

$$\text{BW at } f_o = 4.25 \text{ GHz} < \text{BW at } f_1 = 9.25 \text{ GHz, for } w_o = 0.5 \text{ mm} \quad (3)$$

To further enhance the performance of single-stage dual-band bandpass filter stopband behavior, the ECC configuration method was introduced in this design as shown in Figure 3(b). Three single-stages dual-band bandpass filter with various gap size L_{g2} were designed to identify the effect of ECC. Its S_{21}-magnitude under the three different gap size L_{g2} is simulated and plotted in Figure 5 to demonstrate the behavior of filter on stopband between dual-band at f_o = 4.25 GHz and f_1 = 9.25 GHz. It clearly shows that as the gap size L_{g2} decreases the stopband behavior improves and when L_{g2} = 0.1 mm, the filter shows excellent stopband performance with two transmission zero frequencies between the two operating frequencies. The ECC technique was introduced in the design of PCML-SIR dual-band bandpass filter.

4. Dual-Band PCML-SIR ECC Filter

Two-stage dual-band PCML-SIR bandpass filter with various configurations as shown in Figure 6 with ECC configuration has been designed. Their dual-band performances such as insertion loss, bandwidth and stopband performance were effectively controlled by the feeding network width and the gap size of edge capacitive coupling. From the above discussion, the PCML-SIR filter with small width feeding network and small gap size of edge capacitive coupling giving good bandwidth at both bands with excellent stopband performances. To further realize two-stage dual-band PCML-SIR bandpass filter with excellent performance the respective design were repeated with various controllable physical parameters. Each and every physical parameter shown in Figure 6, carefully adjusted for the better performance of the filter.

After optimization design is carried out to achieve excellent dual-band and stopband performance, the three dual-band filters with various coupling length were fabricated. Figure 7 shows the simulated and measured frequency responses for an optimized dual-band PCML-SIR bandpass filter. It can be observed that the simulated and measured insertion and return loss response are almost identical over the frequency range. The filters show excellent dual-band performance with improved stopband performance. Overall the stopband exhibits less than -50 dB low insertion losses with two transmission zero frequency. It shows that a cost effective compact dual-band PCML-SIR filter with excellent passband and stopband response can be realized by using edge capacitive coupling.

5. Conclusion

In this paper, a dual-band bandpass filter with adjustable bandwidth and improved stopband performances proposed and fabricated by using the PCML-SIR edge capacitive coupling configuration. The overall performance of the filter depends on the feeding network width and gap size of edge capacitive coupling. Feeding network width of PCML structure is used as the main components to improve the second band bandwidth. Meanwhile the gap size of edge capacitive coupling was used to improve the stopband characteristics. Overall the single-stage dual-band bandpass filter with edge capacitive coupling configuration and narrow feeding networks shows excellent results in terms of bandwidth and stopband characteristics. Further, the PCML-SIR dual-band bandpass filter with edge capacitive coupling configuration optimally design and verified by experiments. The simple and compact design of PCML-SIR dual-band bandpass filter by edge capacitive coupling configuration give excellent results. The resulting agreement between measurements and simulations has confirmed the experimental viability of the edge capacitive coupling configuration for dual-band design.

References

[1] M.-L. Chuang, "Concurrent dual band filter using single set of microstrip open-loop resonators", Electronics Letters, vol. 41, No.18, September 2005.

[2] Shen Sun, Lei Zhu, "Compact Dual-Band Microstrip Bandpass Filter Without External Feeds", IEEE Microwave and Wireless Components Letters, vol. 15, No. 10, pp. 644- 646, October 2005.

[3] J. Wang, Y.-X. Guo, B.-Z Wang, L.C. Ong and S. Xiao, "High-selectivity dual-band stepped-impedance bandpass filter", Electronics Letters, vol. 42, No.9, April 2006.

[4] Cheng-Chung Chen, "Dual-Band Bandpass Filter Using Coupled Resonator Pairs", IEEE Microwave and Wireless Components Letters, vol. 15, No. 4, pp. 259 - 261, April 2005.

[5] Jayaseelan Marimuthu and Mazlina Esa, "Equivalent J – Inverter Network Parameters Analysis and Cancellation of Spurious Response of Parallel Coupled Microstrip Line", *Proceedings of IEEE 2006 Int. RF and Microwave Conference* September 12-14, 2006.

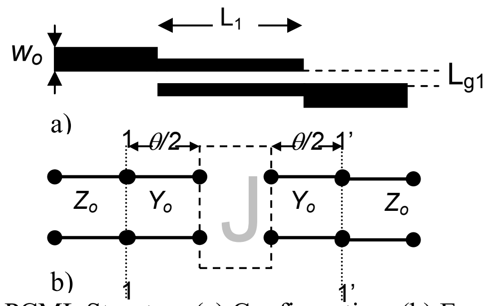

Figure 1: A PCML Structure (a) Configuration, (b) Equivalent J-inverter.

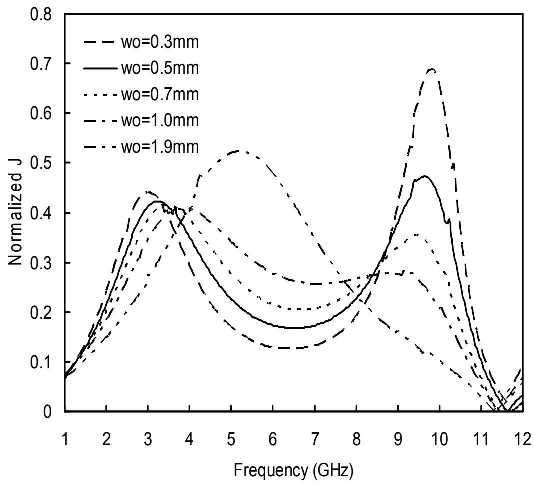

Figure 2: Frequency – Dispersive Normalized J Susceptance of Figure 1a with various w_o.

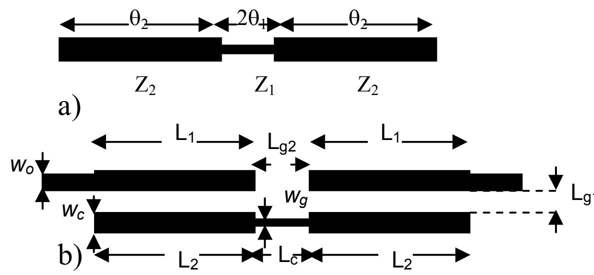

Figure 3: a) Simple SIR Structure, b) Single-Stage Dual-Band SIR-PCML Bandpass Filter with Edge Capacitive Coupling Configuration

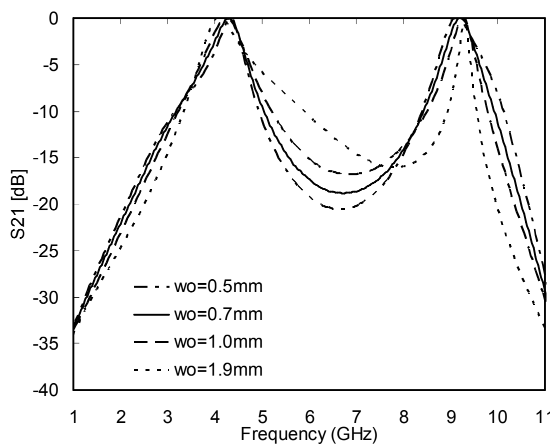

Figure 4: S_{21}-magnitude of a single-stage dual-band PCML-SIR with varying w_o.

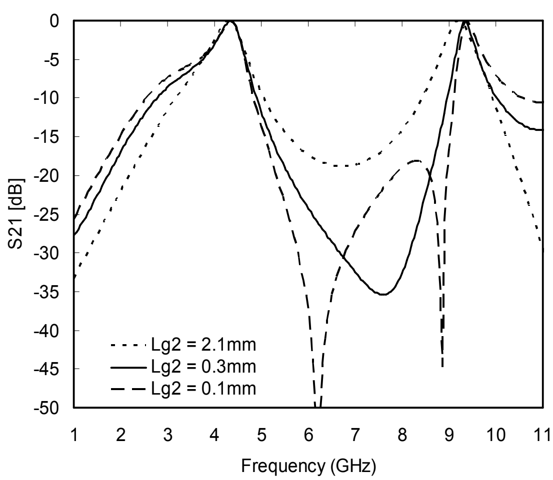

Figure 5: S_{21}-magnitude of a single-stage dual-band PCML-SIR with varied capacitive gap L_{g2}.

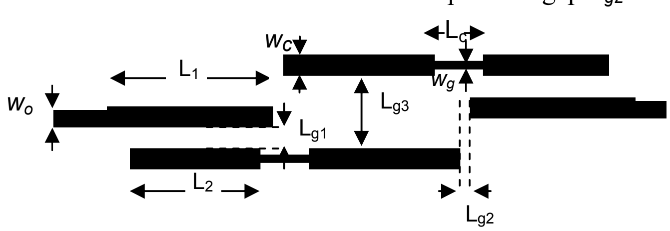

Figure 6: The proposed edge capacitive coupling configuration of PCML-SIR dual-band bandpass Filter

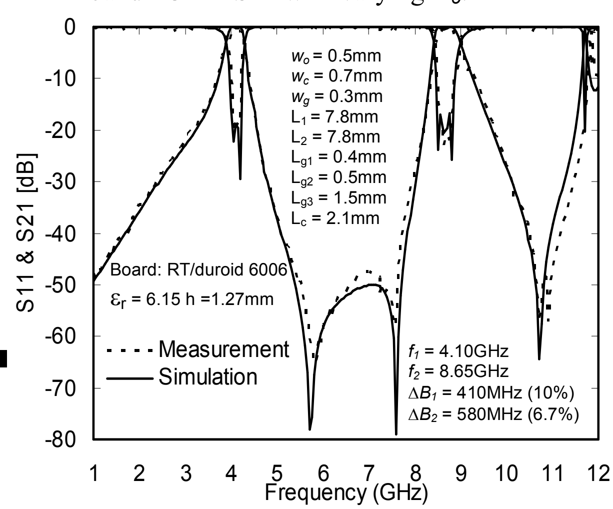

Figure 7: Simulated and measured results of the two-stage dual-band PCML-SIR ECC configuration.